

Quantitative Structure-activity Relationship Studies and Nonlinear Optical Properties of 2-Phenylbenzofuran Derivatives: A Density Functional Theory Study

N. Benhalima^a, M. Touhami^b, F. Khelifaoui^{c,*}, F. Yahia Cherif^b and A.K. Chouaih^d

^aLaboratory of Chemistry: Synthesis, Properties and Applications (LCSPA), Faculty of Sciences, University of Saida-Dr. Moulay Tahar, Saida, Algeria

^bModeling and Calculation Methods Laboratory, University of Saida-Dr. Moulay Tahar, Saida, Algeria

^cLaboratory of Physico-Chemical Studies, University of Saida-Dr. Moulay Tahar, Saida, Algeria

^dLaboratory of Technology and Solid Properties (LTSP), Abdelhamid Ibn Badis University of Mostaganem, Mostaganem, Algeria

(Received 20 June 2021, Accepted 28 August 2021)

Density functional theory (DFT) calculations were performed in the ground state of 2-phenylbenzofuran using the GGA-PBE, PBV86, and meta-GGA TPSS hybrid functionals with the 6-31G(d,p) basis set. First, theoretical calculations were performed using the above functionals to obtain the stable conformer of the molecule. In addition, Mulliken population, natural population, and natural bond orbital analyses were carried out. The molecular electrostatic potential, band gap energies, global and local reactivity descriptors, and nonlinear optical (NLO) properties were studied. Additionally, the NLO properties of 2-phenylbenzofuran and those of its derivatives were investigated by the GGA-PBE/6-31G(d,p) level of theory. The first-order hyperpolarizability of all 2-phenylbenzofuran derivatives was found to be varying from 4.00×10^{-30} to 43.57×10^{-30} (esu), indicating that they possess remarkable NLO properties. In addition, a multiple linear regression model was used to model the relationships between molecular descriptors and the activity of 2-phenylbenzofuran derivatives. Quantitative structure-activity relationship (QSAR) studies were performed using quantum chemical descriptors. The QSAR was applied to determine the relationship between various physico-chemical parameters of the studied compounds and their biological activities. The statistical quality of the QSAR models was assessed using statistical parameters, *i.e.*, R^2 , R^2_{adj} , and R^2_{cv} .

Keywords: NLO, NBO, 2-Phenylbenzofuran, MLR, QSAR

INTRODUCTION

Benzofuran, as an important heterocyclic compound, is found abundantly in natural products as well as in synthetic materials. Benzofuran derivatives have drawn the attention of many researchers due to their pharmacological properties, such as antibacterial, antifungal [1], antitumor, antiviral [2], and antimicrobial [3] activities. Researchers have also found that benzofuran derivatives can be used as antitubercular [4], anti-HIV [5], anti-inflammatory,

analgesic, antipyretic [6], anti-Alzheimer [7], hypotensive, antiarrhythmic [8], and antiprotozoal [9-11] agents. Benzofuran derivatives, with two-electron donor-acceptor groups, are connected by a π -conjugation bridge, which provides a pathway for the redistribution of the electron density (EM) under the influence of an external field. Moreover, these derivatives are molecules of great importance in materials chemistry [12]. Over the last few years, the benzofuran derivatives, due to their strong chemical stability, have attracted the attention of a great number of researchers in the field of optical sensing, optical data storage, LED, and solar cells [13] and have been considered for use in electroluminescent materials [14],

*Corresponding author. E-mail: friha.khelifaoui@univ-saida.dz

sensors [15], lasers, and other optoelectronic devices. It is worth noting that benzofuran derivatives are promising candidates for studying nonlinear optical (NLO) properties [16]. Maridevarmath *et al.* investigated the synthesis, photophysical characterization, solvent effect, and density functional theory (DFT) studies of a biologically active benzofuran derivative, *i.e.* (5-methyl-benzofuran-3-yl)-acetic acid hydrazide [17]. Hiremath *et al.* conducted an experimental and computational study on the structural and spectroscopic characterization of 2-(5-methyl-1-benzofuran-3-yl) acetic acid in a monomer-dimer system and attempted to identify its specific reactive and drug-likeness properties [18]. Similarly, Murthy *et al.* reported on the structural and spectroscopic characterization, reactivity study, and charge transfer analysis of the newly synthesized 2-(6-hydroxy-1-benzofuran-3-yl) acetic acid [19]. Furthermore, Hasan *et al.* investigated the structural, vibrational, and NLO behavior of 4b,9b-dihydroxy-7,8-dihydro-4bH-indeno[1,2-b]benzofuran-9,10(6H,9bH)-dione using a DFT study [20]. DFT is currently viewed as one of the most successful computational chemistry approaches because it yields accurate results for several physico-chemical properties of chemical, physical, and biological systems, especially when hybrid DFT hybrid functionals are used. DFT offers reliable information about the excited-state properties of small molecules, donor and acceptor systems, and metal complexes [21-23]. The GGA-PBE functional has previously been shown to provide an optimum compromise between the experimental and computational calculations obtained by molecular geometries, vibrational frequencies, atomic charges, global reactivity descriptors (GRDs), thermodynamic properties, and especially NLO properties for large and medium-sized molecules [24-27]. Quantum-chemical methods enable the definition of a large number of parameters characterizing the reactivity, form, and binding properties of a molecule and its fragments and substituents. Due to the importance of the information encoded in many theoretical quantities, the use of quantum-chemical descriptors in the development of a quantitative structure-activity relationship (QSAR) model has two main advantages: First, the compounds and their various fragments and substituents can be characterized directly and only based on their molecular structures; secondly, the proposed mechanism of action can be directly explained in

terms of the chemical reactivity of the compounds under study. Several researchers have studied the application of quantum-chemical descriptors in QSAR studies. The use of DFT to calculate these descriptors is justified by the fact that some comparative QSAR studies have shown that DFT can improve the accuracy and reliability of QSARs [28-31]. The present work aimed to examine the relationship between *in vitro* antiprotozoal activities of 49 2-phenylbenzofuran derivatives, which have been recently identified by Stanislav *et al.* [10] and are listed in Table 8, against *Plasmodium falciparum* and cytotoxicity in mammals.

The main objective of using statistics is to reduce uncertainty and extract useful information from data through the analysis of variations in observations. Data analysis is used to describe, understand, and control the studied phenomena.

Developing QSAR models is not easy. The first difficulty lies in the difference between the scales used to analyze correlated data and those used to analyze predicted data. The former group of scales functions at the molecular level while the latter group functions at the macroscopic level [32]. In fact, many approaches have been proposed to develop a reliable model from the available data. In each case, there are usually several approaches available, but it is necessary to choose the one that allows a more accurate and detailed characterization of the system under study. Molecular modeling methods are computer tools that can be used to explore the relationships between molecular descriptors, calculated from chemical structures, and experimentally determined properties. In general, linear functions can be easily interpreted and are sufficiently precise for modeling a small series of identical compounds, especially when the descriptors are carefully selected for a given quantity. One of these linear functions is multiple linear regression (MLR), which is based on the assumption that there is a linear relationship between a dependent variable (Y) and a series of (n) independent variables (X_i) [33]. The objective is to obtain an equation of the form $Y = a_0 + a_1X_1 + a_2X_2 + a_3X_3 + \dots + a_nX_n$, where $X_1 \dots X_n$ are molecular descriptors with their assigned coefficients $a_1 \dots a_n$. Any QSAR model should be properly validated before being used to interpret and predict the biological responses of compounds. Several methods are used to assess

the validity of QSAR models. These include randomization of response data into reordered response vectors, cross-validation, splitting of chemical compounds into a training and validation set, and confirmation using an independent external validation set [34-37]. QSAR models were generated using MLR in Minitab software [38]. Then, the generated models were evaluated using R^2 and adjusted R^2_{adj} coefficients.

The molecular structural parameters, potential energy surface (PES), HOMO-LUMO energies, charge distribution (Mulliken population analysis [MPA], natural population analysis [NPA]), total dipole moment (μ), polarizability (α), first-order hyperpolarizability (β), GRDs, and local reactivity descriptors (LRDs) were also calculated to better understand the reactive nature of the study compounds. In this study, all theoretical calculations were performed using the DFT method with GGA-PBE, PBV86, and meta-GGA-TPSS functionals in conjunction with the 6-31G(d,p) basis set for 2-phenylbenzofuran. The most accurate functional was found to be GGA-PBE. Hence, the NLO properties and all descriptors for 2-phenylbenzofuran derivatives were calculated using the same functional (*i.e.*, GGA-PBE).

COMPUTATIONAL METHODS

In this study, the DFT was used, and the 3D molecular structures were generated using GaussView 3.0 [39]. It is worth noting that all calculations were performed using the Gaussian 09 program package [40]. In addition, the geometry optimization of 2-phenylbenzofuran was performed using GGA-PBE (with the exchange functional developed by Perdew, Burke, and Ernzerhof) [41], BPV86 (with the functional developed by Burke and Perdew and the correlation introduced by Vosko *et al.*) [42], meta-GGA-TPSS [43,44], and the 6-31G(d,p) basis set [45]. All properties of 2-phenylbenzofuran derivatives were calculated using HyperChem 8.0.3 software (Hypercube, Inc, Gainesville, Florida, USA) and Gaussian 09 program package. The geometries of the 2-phenylbenzofuran derivatives were optimized using hybrid DFT/GGA-PBE functional with the 6-31G(d,p) basis sets in Gaussian 09. The optimization was performed to find a geometry structure with minimal energy and extract a set of quantum chemistry descriptors, including the energy of the highest

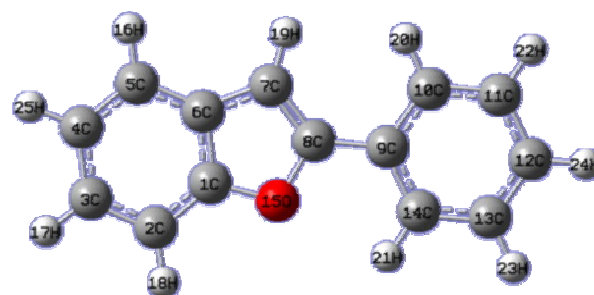


Fig. 1. Molecular structure of 2-phenylbenzofuran, along with the atom numbering.

occupied molecular orbit (E_{HOMO}), natural charge, bond lengths, first-order hyperpolarizability, entropy, and zero-point vibrational energy (ZPVE). The calculation of the properties, including the log of the octanol-water partition coefficient and hydration energy, which is a key factor in determining the stability of different molecular conformations and is reversely correlated with the size of molecules, was performed using the QSAR properties module implanted in HyperChem.

RESULTS AND DISCUSSION

Geometry Description of 2-Phenylbenzofuran

The optimized structures of 2-phenylbenzofuran were calculated at the GGA-PBE, PBV86, and meta-GGA-TPSS levels using the 6-31G(d,p) basis set. These computations were conducted using the Gaussian 09 program package and are illustrated in Fig. 1. No symmetry constraint was imposed on the geometry optimization, and the structure was verified to be the local minimum using frequency analysis. The theoretical calculations were performed on an isolated molecule in the gas phase. In this work, the optimization of geometric parameters of 2-phenylbenzofuran was carried out without imposing any molecular symmetry constraints. In addition, the comparative optimized structural parameters, such as bond lengths and bond angles, are presented in Table 1 (see supplementary material). The obtained geometric parameters at all levels of theory were found to be in reasonable agreement with the available crystallographic data [46].

Table 1. Bond Lengths (in Å) and Valence Angles (in Degrees) of 2-Phenylbenzofuran

Bond lengths	Exp. ^a	GGA-PBE	BPV86	meta-GGA-TPSS
C1-C2	1.384	1.394	1.394	1.393
C2-C3	1.384	1.402	1.403	1.401
C3-C4	1.399	1.413	1.414	1.413
C4-C5	1.380	1.398	1.390	1.397
C5-C6	1.400	1.411	1.412	1.410
C6-C1	1.397	1.418	1.418	1.415
C6-C7	1.435	1.436	1.438	1.437
C7-C8	1.361	1.379	1.379	1.376
C8-C9	1.456	1.458	1.458	1.458
C9-C10	1.411	1.414	1.415	1.413
C10-C11	1.384	1.397	1.398	1.396
C11-C12	1.394	1.404	1.405	1.403
C12-C13	1.384	1.402	1.403	1.401
C13-C14	1.386	1.399	1.399	1.398
C14-C9	1.398	1.414	1.414	1.412
O-C1	1.372	1.373	1.375	1.376
O-C8	1.392	1.391	1.393	1.394
Valence angles				
C1-O-C8	106.31	106.57	106.58	106.51
O1-C1-C6	110.34	110.35	110.31	110.27
O1-C1-C2	125.51	125.81	125.82	125.75
C2-C1-C6	124.14	123.84	123.87	123.98
C1-C2-C3	115.87	116.31	116.30	116.21
C2-C3-C4	121.74	121.34	121.34	121.36
C3-C4-C5	121.31	121.46	121.46	121.47
C4-C5-C6	118.36	118.37	118.38	118.34
C5-C6-C1	118.58	118.67	118.65	118.64
C5-C6-C7	135.74	135.94	135.93	135.88
C1-C6-C7	105.67	105.39	105.42	105.48
C6-C7-C8	107.07	106.98	107.04	107.10
C7-C8-O	110.6	110.72	110.66	110.64
C9-C8-O	114.61	116.29	116.28	116.08
C7-C8-C9	134.67	132.99	133.06	133.27
C8-C9-C10	121.89	120.50	120.50	120.50
C8-C9-C14	119.94	120.83	120.84	120.79
C10-C9-C14	118.17	118.68	118.66	118.71
C9-C10-C11	120.31	120.56	120.57	120.54
C10-C11-C12	120.13	120.36	120.36	120.35
C11-C12-C13	120.42	119.51	119.51	119.53
C12-C13-C14	119.38	120.45	120.46	120.45
C13-C14-C9	121.56	120.44	120.44	120.42

^a[2-(2-Methoxyphenyl)-1-benzofuran] [46].

The energies of the structure of 2-phenylbenzofuran optimized with the GGA-PBE, BVP86, and meta-GGA-TPSS functionals were -613.99, -614.78, and -614.87 (u.a), respectively. These values indicate that the meta-GGA-TPSS method, at the 6-31G(d,p) level, could better predict the minimum energy configuration for this compound compared with the other two methods. Table 1 indicates that most of the calculated bond lengths and bond angles were only slightly different from the experimental ones. It can be stated that the experimental results are dependent on the solid phase whereas the calculated ones are dependent on the isolated gas phase. The dihedral angle, between the benzofuran and phenyl rings, was found to be 0.27°, 0.29°, and 0.27° for GGA-PBE, BVP86, and meta-GGA-TPSS, respectively. Moreover, it is worth mentioning that 2-phenylbenzofuran exhibited a pseudo-planar geometry. Table 1 shows a good agreement between the predicted and experimental results. Therefore, it can be concluded that the DFT/GGA-PBE method is suitable for calculating the properties of 2-phenyl Benzofuran derivatives.

Population Charge Analysis of 2-Phenylbenzofuran

Atomic charges. The charge distribution was studied

using two types of population analyses, namely, MPA and NPA. Population analyses are mathematical approaches used for the partitioning of the electronic density to calculate atomic charges, bond orders, and other related properties. Atomic charges, which were calculated by MPA and NPA, play an important role in quantum chemical calculations of molecular systems due to their effect on the dipole moment, molecular polarizability, electronic structure, NLO properties, and several other molecular properties [47,48]. The MPA and NPA atomic charges of the non-H atoms of 2-phenylbenzofuran were calculated at GGA-PBE, PBV86, and meta-GGA-TPSS levels with the 6-31G(d,p) basis set, and the obtained results are summarized in Table 2 (see supplementary material). The graphical results are illustrated in Fig. 2. MPA and NPA were obtained from the optimized geometry and natural bond orbital (NBO) analysis, respectively. It is widely acknowledged that both methods (*i.e.*, MPA and NPA) predict similar tendencies, except for C6 and C9 atoms. In MPA, it is assumed that all hydrogen atoms have positive charges, so all carbon atoms bonded to these electropositive atoms must have negative charges, except for C1, C6, C8, and C9 atoms that have positive charges and thus are more

Table 2. Net Charges of 2-Phenylbenzofuran Calculated by MPA and NPA

	GGA-PBE		PBV86		meta-GGA-TPSS	
	Mulliken	NPA	Mulliken	NPA	Mulliken	NPA
C1	0.310	0.307	0.312	0.309	0.325	0.312
C2	-0.136	-0.287	-0.141	-0.285	-0.149	-0.273
C3	-0.117	-0.249	-0.118	-0.248	-0.127	-0.238
C4	-0.105	-0.261	-0.105	-0.260	-0.115	-0.251
C5	-0.155	-0.232	-0.161	-0.230	-0.162	-0.219
C6	0.072	-0.117	0.086	-0.116	0.063	-0.119
C7	-0.162	-0.299	-0.172	-0.297	-0.171	-0.287
C8	0.254	0.304	0.259	0.306	0.272	0.310
C9	0.038	-0.106	0.050	-0.105	0.032	-0.106
C10	-0.111	-0.217	-0.116	-0.216	-0.123	-0.206
C11	-0.111	-0.245	-0.111	-0.244	-0.120	-0.234
C12	-0.091	-0.245	-0.092	-0.243	-0.102	-0.233
C13	-0.104	-0.243	-0.105	-0.241	-0.114	-0.232
C14	-0.114	-0.221	-0.120	-0.220	-0.123	-0.209
O15	-0.493	-0.429	-0.503	-0.435	-0.527	-0.449

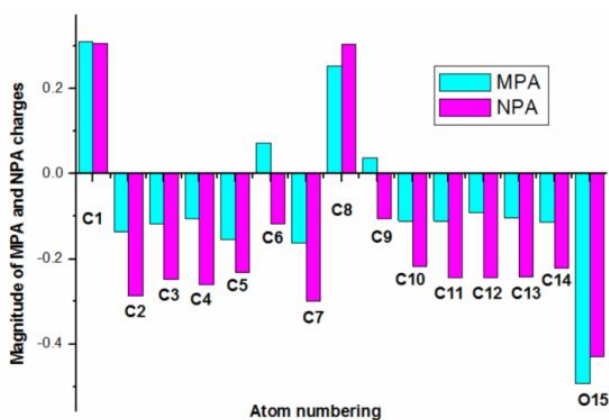


Fig. 2. MPA and NPA of 2-phenylbenzofura.

prone to nucleophilic attack.

Natural bond orbital (NBO) analysis. The second-order Fock matrix was used to evaluate the donor-acceptor interactions in the NBO basis set [49]. These interactions resulted in the loss of occupancy from the localized NBO of the idealized Lewis structure into an empty vacant non-Lewis orbital. For each donor (i) and acceptor (j), the stabilization energy $E^{(2)}$ related to the delocalization $i \rightarrow j$

was approximated using the following equation:

$$E^{(2)} = \Delta E_{ij} = q_i \frac{F_{ij}^2}{\varepsilon_j - \varepsilon_i} \quad (1)$$

where ΔE_{ij} is the decrease in the perturbation energy, q_i is the donor orbital occupancy, ε_i and ε_j are diagonal elements indicating the donor and acceptor orbital energies, and F_{ij} is the off-diagonal NBO Fock matrix element. The NBO analysis of 2-phenylbenzofuran was performed at the GGA-PBE/6-31G(d,p) level, and the obtained results are summarized in Table 3. The second-order perturbation energies between the high-energy Lewis-type NBOs (donors) and the low energy non-Lewis-type NBOs (acceptors) ($E^{(2)}$), electron density (ED), donors and acceptors, energy difference ($\varepsilon_j - \varepsilon_i$), and polarization energy (F_{ij}) of 2-phenylbenzofuran are also presented in Table 3. The high value of $E^{(2)}$ indicates stronger interactions [50]. For 2-phenylbenzofuran, hyperconjugative interactions are attributed to the delocalization of electrons from σ and n to σ^* , and from π , n , and π^* to π^* . Moreover, the NBO analysis allows the description of the bonding in terms of

Table 3. Second-Order Perturbation Theory Analysis of Fock Matrix in NBO Basis of 2-Phenylbenzofuran

Donor (i)	ED ϵ (e)	Acceptor (j)	ED (e)	$E^{(2)}$ (Kcal mol ⁻¹)	$E(j) - E(i)$ (a.u)	$F(i,j)$ (a.u)
$\pi(C1-C6)$	1.59	$\pi^*(C2-C3)$	0.34	13.92	0.23	0.05
$\pi(C1-C6)$		$\pi^*(C4-C5)$	0.31	13.59	0.24	0.052
$\pi(C1-C6)$		$\pi^*(C7-C8)$	0.30	12.08	0.23	0.048
$\pi(C2-C3)$	1.71	$\pi^*(C1-C6)$	0.48	15.94	0.23	0.056
$\pi(C2-C3)$		$\pi^*(C4-C5)$	0.31	13.72	0.23	0.051
$\pi(C4-C5)$	1.72	$\pi^*(C1-C6)$	0.48	14.07	0.22	0.053
$\pi(C4-C5)$		$\pi^*(C2-C3)$	0.34	14.45	0.23	0.052
$\pi(C7-C8)$	1.81	$\pi^*(C1-C6)$	0.48	11.42	0.24	0.051
$\pi(C7-C8)$		$\pi^*(C9-C14)$	0.39	11.67	0.24	0.05
$\pi(C9-C14)$	1.62	$\pi^*(C7-C8)$	0.30	16.81	0.22	0.056
$\pi(C9-C14)$		$\pi^*(C10-C11)$	0.31	14.39	0.23	0.052
$\pi(C9-C14)$		$\pi^*(C12-C13)$	0.34	14.86	0.23	0.052
$\pi(C10-C11)$	1.68	$\pi^*(C9-C14)$	0.39	14.18	0.23	0.052
$\pi(C10-C11)$		$\pi^*(C12-C13)$	0.34	14.27	0.23	0.052
$\pi(C12-C13)$	1.66	$\pi^*(C9-C14)$	0.39	14.89	0.23	0.053
$\pi(C12-C13)$		$\pi^*(C10-C11)$	0.31	14.75	0.23	0.052
$n2(O15)$	1.72	$\pi^*(C1-C6)$	0.48	22.01	0.29	0.075
$n2(O15)$		$\pi^*(C7-C8)$	0.30	22.91	0.28	0.072

the natural hybrid orbital (NHO) with higher- and lower-energy orbitals. In the NBO analysis, large $E^{(2)}$ values indicate intensive interactions between electron donors and electron acceptors.

In the benzofuran ring, the intramolecular interactions, due to the orbital overlap, take place between π (C1-C6)/ π^* (C2-C3)/ π^* (C4-C5)/ π^* (C7-C8) (13.92/13.59/12.08 kJ mol⁻¹), π (C2-C3)/ π^* (C1-C6)/ π^* (C4-C5) (15.94/13.72 kJ mol⁻¹), π (C4-C5)/ π^* (C1-C6)/ π^* (C2-C3) (14.07/14.45 kJ mol⁻¹), and π (C7-C8)/ π^* (C1-C6) (11.42 kJ mol⁻¹). All these transitions take place within the benzofuran ring while transitions π (C9-C14)/ π^* (C10-C11)/ π^* (C12-C13) (14.39/14.86 kcal mol⁻¹), π (C10-C11)/ π^* (C9-C14)/ π^* (C12-C13) (14.18/14.27 kcal mol⁻¹), π (C12-C13)/ π^* (C9-C14)/ π^* (C10-C11) (14.89/14.75 kcal mol⁻¹) occur in the phenyl ring. In addition, major interactions occur between the lone pairs of n2 (O15)/ π^* (C1-C6)/ π^* (C7-C8) (22.01/22.91 kcal mol⁻¹).

Molecular Electrostatic Potential (MEP) Analysis of 2-Phenylbenzofuran

The 3D-MEP and electron density (ED) of the optimized molecular structure of 2-phenylbenzofuran were calculated using the GGA-PBE/6-31G(d,p) functional, as shown in Fig. 3. The MEP of compounds shown in Fig. 3 increases in the following order: red < orange < yellow < green < blue (dark blue). It is worth noting that the blue color represents regions with the most positive electrostatic potential, thus having the strongest attraction. However, the red color represents regions with the most negative electrostatic potential, thus having the strongest repulsion. The negative (red, orange, and yellow) regions of the MEP are related to electrophilic reactivity [51]. Furthermore, the 3D graph shows that the region close to the oxygen atom is rich in electrons due to the red color. In the compound under consideration, the hydrogen atoms (blue region) are expected to react with nucleophilic sites.

Electronic Properties

Analysis of frontier molecular orbitals (FMOs). The frontier orbitals HOMO and LUMO are important factors in quantum chemistry because they determine how a molecule interacts with other species. Furthermore, the frontier orbital gap facilitates the characterization of the chemical reactivity

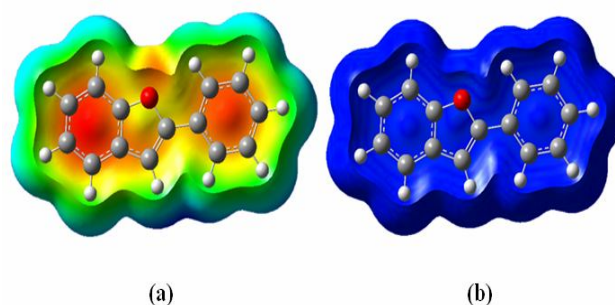


Fig. 3. a) Two-dimensional molecular electrostatic potential (MESP) and b) electron density (ED) for 2-phenylbenzofuran.

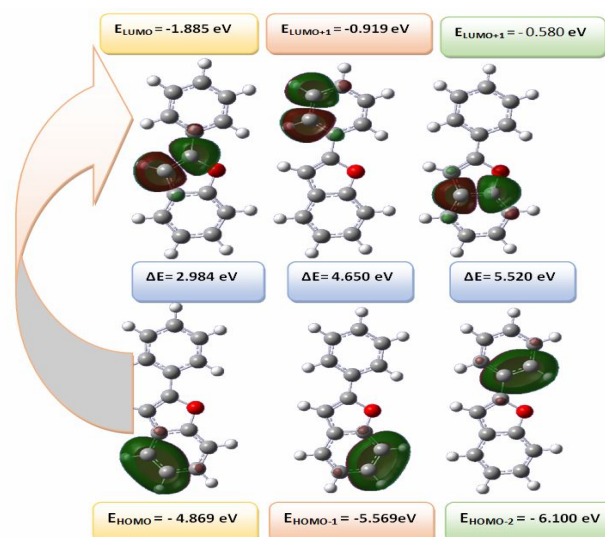


Fig. 4. HOMO-LUMO plot of 2-phenylbenzofuran.

and kinetic stability of the molecule. It is widely acknowledged that a molecule with a small frontier orbital gap, also known as a soft molecule, is more polarizable than other molecules and generally has a high chemical reactivity and low kinetic stability. The small energy gap between HOMO and LUMO facilitates the intramolecular charge transfer, which, in turn, makes the material to be NLO active. The HOMO and LUMO energies and energy gap ($\Delta E = E_{\text{HOMO}} - E_{\text{LUMO}}$ (eV)) of 2-phenylbenzofuran were calculated using the GGA-PBE, BVP86, and meta-GGA-TPSS functionals with the 6-31G(d,p) basis set. The corresponding plot is shown in Fig. 4, and the computed

Table 4. The Calculated Values of Quantum Chemical Reactivity Descriptors, Dipole Moment μ (D), Polarizability α ($\times 10^{-23}$ esu), and First-Order Hyperpolarizability β ($\times 10^{-30}$ esu) for 2-Phenylbenzofuran

Parameters	GGA-PBE	BVP86	meta-GGA-TPSS
E_{HOMO} (eV)	-4.869	-4.960	-4.855
E_{LUMO} (eV)	-1.885	-1.982	-1.760
$E_{\text{HOMO}}-E_{\text{LUMO}}$ (eV)	2.984	2.978	3.095
Ionization potential IP (eV)	4.869	4.960	4.855
Electron affinity EA (eV)	1.885	1.982	1.760
Electronegativity χ (eV)	3.377	3.471	3.307
Chemical hardness η (eV)	1.492	1.489	1.548
Electrophilicity index ω (eV)	3.822	4.046	3.534
μ (D)	0.99	1.01	0.501
α . 10^{-23} (esu)	2.48	2.49	2.46
β . 10^{-30} (esu)	7.30	7.23	6.87

Table 5. The UV-Vis Wavelength (λ) and Oscillator Strengths (f) of 2-Phenylbenzofuran in Gas and Solvent Phases

	Excited state	λ (nm)	Energy (eV)	f(O.S)	Major contributions
GGA-PBE	S1 (Gas)	327.14	3.7899	0.586	HOMO->LUMO (92%)
	(Water)	334.78	3.7034	0.795	HOMO->LUMO (97%)
PBV86	S1 (Gas)	327.94	3.7806	0.594	HOMO->LUMO (92%)
	(Water)	335.57	3.6947	0.799	HOMO->LUMO (97%)
meta-GGA-TPSS	S1 (Gas)	319.57	3.8797	0.638	HOMO->LUMO (94%)
	(Water)	327.21	3.7891	0.832	HOMO->LUMO (94%)

values are presented in Table 4. The energy gap values obtained using GGA-PBE, BVP86, and meta-GGA-TPSS functionals were 2.984, 2.978, and 3.095 eV, respectively. GGA-PBE and BVP86 functionals, compared to meta-GGA-TPSS functional, showed lower energy gap values. These small energy gap values indicate that 2-phenylbenzofuran is highly reactive and thus can be a promising candidate for NLO applications.

UV-Vis spectral analysis. To determine the nature of electronic transitions, the electronic spectra of the studied molecule were calculated using time-dependent density-functional theory (TDDFT) [52] at the GGA-PBE, BVP86, and meta-GGA-TPSS levels on the basis of the optimized ground-state structure. Calculations were performed in

water using the conductor-like polarizable continuum model (CPCM) [53]. The major contributions of HOMO-LUMO transitions were analyzed using Gauss-Sum 2.2 software package [54]. The calculated absorption wavelength λ (nm), oscillator strengths (f), and excitation energies (eV), along with their assignments and contributions, are given in Table 5. The theoretical UV-Vis spectra of 2-phenylbenzofuran are shown in Fig. 5. The corresponding theoretical wavelengths were 327.14 nm ($f=0.5859$) in the gas phase and 334.78 nm ($f=0.7950$) in the solvent phase.

Reactivity Descriptors of 2-Phenylbenzofuran

Global reactivity descriptors (GRDs). To investigate the chemical reactivity of 2-phenylbenzofuran, GRDs were

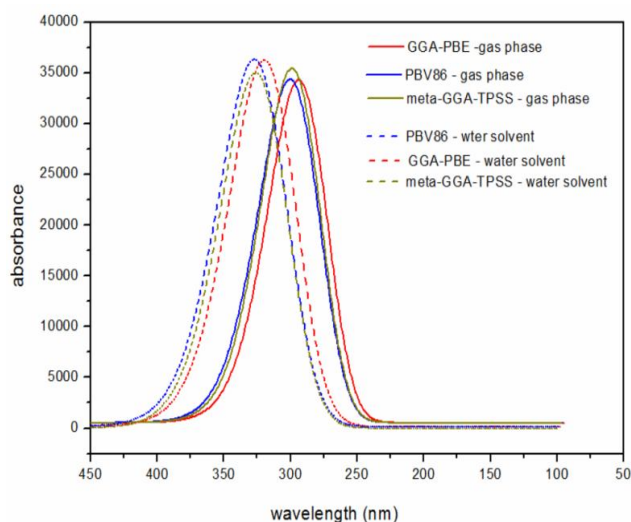


Fig. 5. The theoretical UV-Vis spectra of 2-phenylbenzofuran in gas and solvent phases.

estimated using the HOMO-LUMO energies. The chemical reactivity of the molecular systems was determined using Koopmans' theorem [55,56]. The above-mentioned descriptors were calculated using the following equation:

$$\chi = \left(\frac{IP + EA}{2} \right), \eta = \frac{1}{2} \left(\frac{IP - EA}{2} \right), \omega = \mu^2 \quad (2)$$

where $IP = -E_{\text{HOMO}}$ and $EA = -E_{\text{LUMO}}$ are the ionization potential and electron affinity, respectively. The GRDs were evaluated using GGA-PBE, BVP86, and meta-GGA-TPSS functionals with the 6-31G(d,p) basis set. The computed values are shown in Table 4. The calculated IP and EA of

2-phenylbenzofuran using the GGA-PBE, BVP86, and meta-GGA-TPSS functionals were 4.869, 4.960, and 4.855 eV and 1.885, 1.982, and 1.760 eV, respectively. Chemical hardness (η) is an important property used to measure molecular stability and reactivity and indicates whether the charge transfer occurs within a molecule. The obtained values of η using GGA-PBE, BVP86, and meta-GGA-TPSS functionals were 1.492, 1.489, and 1.548, respectively. According to the results of the GCRD, a high hardness (1.492 eV) value suggests a weak intramolecular charge transfer.

Local reactivity descriptors (LRDs). In order to create a specific reactive site in the molecule, LRDs such as Fukui function (FF) were used. The condensed Fukui functions (f_K^n, f_K^e, f_K^r) were calculated using Hirshfeld atomic charges of neutral, cation and anion states of the title compound [57]. Fukui functions were calculated by the following equations:

$$f_k^m = q_k(N+1) - q_k(N) \rightarrow \text{for nucleophilic attack} \quad (3)$$

$$f_k^e = q_k(N) - q_k(N-1) \rightarrow \text{for electrophilic attack} \quad (4)$$

$$f_k^r = \frac{1}{2}(q_k(N+1) - q_k(N-1)) \rightarrow \text{for radical attack} \quad (5)$$

where q_k is the atomic charge (Mulliken, Hirshfeld, or NBO, etc.) at the k atomic site in the anionic (N+1), cationic (N-1), or neutral (N) molecule. The Fukui functions calculated by NBO charges were found to be in good agreement [58]. The Fukui function values calculated by NBO charges for 2-phenylbenzofuran are tabulated in Table 6. Based on these results, it can be concluded that a

Table 6. Selected Values of the Fukui Functions Calculated by NBO Charges

Atoms	$q_k(N+1)$	$q_k(N)$	$q_k(N-1)$	f_K^n	f_K^e	f_K^r
C1	0.21656	0.30707	0.15158	0.09	-0.155	-0.032
C2	-0.14493	-0.28665	-0.13732	-0.142	0.15	0.004
C3	0.03213	-0.24949	-0.10831	-0.281	0.141	-0.070
C4	-0.14186	-0.26138	-0.15329	-0.119	0.108	-0.005
C8	0.26462	0.30401	0.18911	0.039	-0.115	-0.038
C11	-0.12868	-0.24522	-0.14757	-0.116	0.097	-0.010
C12	0.00489	-0.24474	-0.07029	-0.25	0.175	-0.038
O15	-0.20794	-0.42909	-0.21469	-0.221	0.214	-0.003

nucleophilic attack may occur at carbons C1 and C8; also, an electrophilic attack is equally likely to occur at carbons C2, C4, and C11. The negative Fukui functions for C11, C4, and C2 indicate that it is highly unlikely that a nucleophilic attack occurs on these atoms. However, the results show that the C1 carbon is the most nucleophilic atom. To a lesser extent, the C8 carbon is also prone to a nucleophilic attack. Given that the C8 carbon has the highest value of f_K^e , it can be concluded that it is the most favored site for an electrophilic attack.

Nonlinear Optical (NLO) Activity

NLO properties of 2-phenylbenzofuran. The polarizability (α) and first-order hyperpolarizability (β) were calculated using the x, y, and z components from the Gaussian 09 output according to the following equations [59]:

$$\mu = (\mu_x + \mu_y + \mu_z)^{\frac{1}{2}} \quad (6)$$

$$\alpha_{tot} = \frac{1}{3}(\alpha_{xx} + \alpha_{yy} + \alpha_{zz}) \quad (7)$$

$$\beta = [\beta_x^2 + \beta_y^2 + \beta_z^2]^{\frac{1}{2}} \quad (8)$$

where

$$\beta_x = \beta_{xxx} + \beta_{yyx} + \beta_{zzx}$$

$$\beta_y = \beta_{yyx} + \beta_{yyy} + \beta_{yzz} \quad \text{and}$$

$$\beta_z = \beta_{zzx} + \beta_{zyy} + \beta_{zzz}$$

The polarizability and hyperpolarizability values calculated by Gaussian 09 were converted from atomic units (a.u) into electrostatic units (esu) (α : 1 a.u.= 0.1482×10^{-24} esu; β : 1 a.u. = 8.6393×10^{-33} esu). The μ , α , and the first-order β for the 2-phenylbenzofuran molecule were calculated using the GGA-PBE, BVP86, and meta-GGA-TPSS functionals with the 6-31G(d,p) basis set. The obtained results for NLO properties are listed in Table 4. The molecular dipole moments calculated by the GGA-PBE, BVP86, and meta-GGA-TPSS functionals were 0.99, 1.01, and 0.50 D,

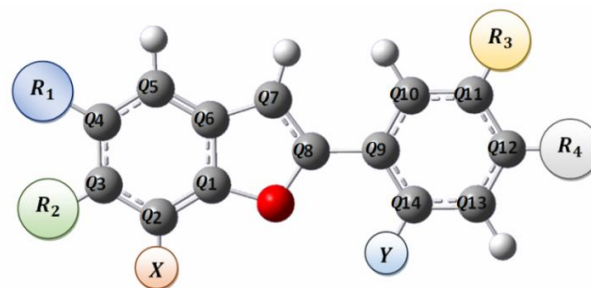


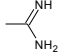
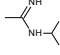
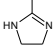
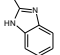
Fig. 6. Structures of 2-Phenylbenzofuran, along with different substituents.

respectively. The calculated α values were equal to 2.48×10^{-23} , 2.49×10^{-23} , and 2.46×10^{-23} esu based on the GGA-PBE, BVP86, and meta-GGA-TPSS functionals, respectively. In addition, the β values of 2-phenylbenzofuran calculated using the GGA-PBE, BVP86, and meta-GGA-TPSS functionals were found to be 7.30×10^{-30} (esu) (32 times that of urea), 7.23×10^{-30} (esu) (31 times that of urea), and 6.87×10^{-30} (esu) (30 times that of urea), respectively. The β value of urea had been reported to be 0.23×10^{-30} (esu) [60]. All these findings suggest that 2-phenylbenzofuran could be a potential candidate for further research aimed at improving NLO properties.

NLO properties of 2-phenylbenzofuran derivatives.

The dipole moments for the 2-phenylbenzofuran derivatives (Fig. 6, Table 7) showed important changes following the changing of the position of the substituents (*i.e.*, Am, *i*-PrAm, Im) (Table 8). The dipole moments of compounds 8 ($R_1 = R_3 = \text{Am}$, $Y = \text{H}$), 29 ($R_1 = R_3 = \text{Am}$, $Y = \text{OCH}_3$), and 35 ($R_1 = R_3 = \text{Am}$, $Y = \text{OH}$) were equal to 5.94, 7.09, and 7.20 D, respectively. It is worth noting that these dipole moments favor intermolecular interactions. Polarizability plays a major role in understanding the electronic charge distribution of a molecule. An external electric field applied to a molecule usually repels the positive charge and attracts the negative charge of the molecule, which, in turn, induces the polarization of the molecule. In the present study, the polarizability values of all the 2-phenylbenzofuran derivatives were calculated, and the obtained results are reported in Table 8. The results in Table 8 show that the α values for the 2-phenylbenzofuran derivatives (1-49) were within the range of $34.70\text{-}70.09 (\times 10^{-24}$ esu). Moreover,

Table 7. Different Substituents Associated with 2-Phenylbenzofuran Derivatives and Experimental Values of Activity

Compounds					X	IM	Cytotox. ^a log(1/IC ₅₀)	P. falcipr. ^b log(1/IC ₅₀)
	R ₁	R ₂	R ₃	R ₄				
1	Am	H	H	Am	H	H	6.279	4.672
2	i-PrAm	H	H	i-PrAm	H	H	8.297	4.863
3	Im	H	H	Im	H	H	7.599	3.000
4	BzIM	H	H	BzIM	H	H	6.826	4.491
5	IM	H	h	IM	H	H	6.519	4.519
6	BzIM	H	H	Im	H	H	6.785	4.602
7	Im	H	H	BzIM	H	H	7.773	4.785
8	Am	H	Am	H	H	H	7.326	4.279
9	i-PrAm	H	i-PrAm	H	H	H	8.299	5.520
10	Im	H	Im	H	H	H	7.530	4.881
11	H	Am	H	Am	H	H	5.903	3.477
12	H	i-PrAm	H	i-PrAm	H	H	8.299	4.176
13	H	Im	H	Im	H	H	6.653	5.037
14	H	Am	Am	H	H	H	8.117	3.602
15	H	i-PrAm	i-PrAm	H	H	H	8.301	4.771
16	H	Im	Im	H	H	H	7.107	5.312
17	Am	H	H	Am	OCH ₃	H	7.487	3.778
18	i-PrAm	H	H	i-PrAm	OCH ₃	H	8.279	4.681
19	Im	H	H	Im	OCH ₃	H	7.299	4.505
20	Am	H	H	Am	OH	H	8.265	4.672
21	i-PrAm	H	H	i-PrAm	OH	H	8.267	4.748
22	Im	H	H	Im	OH	H	8.307	4.342
23	Am	H	H	Am	OH	OH	6.322	4.785
24	i-PrAm	H	H	i-PrAm	OH	OH	8.253	5.491
25	Im	H	H	Im	OH	OH	8.286	4.477
26	Am	H	H	Am	H	OCH ₃	8.196	3.477
27	i-PrAm	H	H	i-PrAm	H	OCH ₃	7.992	4.301
28	Im	H	H	Im	H	OCH ₃	6.869	4.491
29	Am	H	Am	H	H	OCH ₃	8.253	4.602
30	i-PrAm	H	i-PrAm	H	H	OCH ₃	8.253	5.398
31	Im	H	Im	H	H	OCH ₃	7.489	4.813
32	Am	H	H	Am	H	OH	7.522	3.602
33	i-PrAm	H	H	i-PrAm	H	OH	8.262	4.447
34	Im	H	H	Im	H	OH	8.176	3.778
35	Am	H	Am	H	H	OH	8.336	5.899
36	i-PrAm	H	i-PrAm	H	H	OH	8.255	5.713
37	Im	H	Im	H	H	OH	8.299	4.362
38	H	Am	H	Am	H	OCH ₃	8.033	4.301
39	H	i-PrAm	H	i-PrAm	H	OCH ₃	8.258	5.314
40	H	Im	H	Im	H	OCH ₃	6.643	4.886
41	H	Am	Am	H	H	OCH ₃	8.107	4.255
42	H	i-PrAm	i-PrAm	H	H	OCH ₃	8.243	5.467
43	H	Im	Im	H	H	OCH ₃	7.045	4.869
44	H	Am	H	Am	H	OH	8.344	4.845
45	H	i-PrAm	H	i-PrAm	H	OH	8.262	5.776
46	H	Im	H	Im	H	OH	8.286	4.991
47	H	Am	Am	H	H	OH	8.215	5.577
48	H	i-PrAm	i-PrAm	H	H	OH	8.272	5.803
49	H	Im	Im	H	H	OH	8.276	5.013

^aCytotoxicity against mammals. ^bPlasmodium falciparum.

Table 8. The Calculated Values of Electronic Dipole Moment μ (D), Linear Polarizability α ($\times 10^{-24}$ esu), First-Order Hyperpolarizability β ($\times 10^{-30}$ esu), and Energy Gap ΔE (eV) for the 2-Phenylbenzofuran Derivatives Using the GGA-PBE Functional with the 6-31G (d,p) Basis Set

Compounds	μ	α	B	ΔE	Compounds	μ	A	β	ΔE
1	3.51	36.25	14.33	2.760	26	4.27	38.38	15.26	2.762
2	5.35	48.19	25.67	2.755	27	5.48	50.21	27.26	2.734
3	4.21	45.72	18.63	2.516	28	4.91	47.63	22.15	2.583
4	5.24	70.09	4.89	2.415	29	7.09	37.24	9.57	2.988
5	5.50	48.47	6.36	2.487	30	5.64	48.34	10.19	2.912
6	4.73	56.38	40.57	2.532	31	2.62	45.41	5.04	2.839
7	4.24	58.78	23.58	2.391	32	4.19	36.63	18.90	2.746
8	5.94	34.70	9.51	2.953	33	5.49	48.41	31.40	2.726
9	4.59	45.94	11.79	2.791	34	4.85	46.03	27.56	2.538
10	1.36	42.85	4.00	2.706	35	7.20	35.30	10.77	2.971
11	3.76	37.04	19.52	2.624	36	5.57	46.41	12.17	2.881
12	3.41	48.14	18.84	2.585	37	2.06	43.36	4.98	2.822
13	3.17	47.33	34.19	2.382	38	2.81	39.15	19.81	2.643
14	5.57	35.86	9.82	2.775	39	3.22	50.10	17.40	2.628
15	5.19	47.56	11.92	2.773	40	5.44	49.27	36.09	2.420
16	4.72	44.34	17.47	2.559	41	6.63	38.31	7.49	2.825
17	4.20	38.85	17.53	2.776	42	6.28	49.95	8.15	2.802
18	5.90	50.65	27.52	2.753	43	5.90	46.70	13.68	2.662
19	5.06	48.26	21.79	2.546	44	2.60	37.50	24.30	2.616
20	3.91	36.78	15.88	2.767	45	3.49	48.42	21.82	2.606
21	5.71	48.64	25.81	2.741	46	5.25	47.63	43.57	2.394
22	4.74	46.19	19.48	2.558	47	6.75	36.50	9.01	2.793
23	4.23	37.14	19.58	2.751	48	6.14	48.07	11.19	2.784
24	6.10	48.92	31.14	2.706	49	5.97	44.88	17.01	2.625
25	4.98	46.47	27.42	2.555					

Table 8 shows that the highest average alpha amplitudes were 56.38×10^{-24} , 58.78×10^{-24} , and 70.09×10^{-24} (esu), which were related to compounds 6 ($R_1 = \text{BzIM}$, $R_4 = \text{Im}$), 7 ($R_1 = \text{Im}$, $R_4 = \text{BzIM}$), and 4 ($R_1 = R_4 = \text{BzIM}$), respectively. In addition to the dipole moments and polarizability values, the β values of 2-phenylbenzofuran derivatives were estimated at the GGA-PBE/6-31G(d,p) levels of theory. The lowest and highest β amplitudes were 4.00×10^{-30} and 43.57×10^{-30} (esu) for compounds 10 ($R_1 = R_3 = \text{Im}$) and 46 ($R_2 = R_4 = \text{Im}$, $Y = \text{OH}$), respectively.

QUANTITATIVE ANALYSIS of STRUCTURE-ACTIVITY RELATIONSHIPS

The QSAR methods, as the name suggests, are used to establish a mathematical relationship between a molecular structure, encoded by molecular properties called descriptors, and its biological activity using data analysis methods [61]. In this study, we developed predictive models in the following form:

$$\text{Activity} = f(\text{molecular descriptors}) \quad (9)$$

The derived mathematical relationship can then be used as a predictive model to determine the biological activities of new molecules or molecules for which experimental data are not yet available. Such mathematical relationships can also be used to help researchers gain a better understanding of chemical mechanisms and modes of action.

Experimental data. The present theoretical study focused on examining the relationship between the antiprotozoal activities of a series of 2-phenylbenzofuran derivatives, recently identified by Stanislav *et al.*, and some of its descriptors against *Plasmodium falciparum* and cytotoxicity in mammals [10]. The structures of these compounds are summarized in Table 7. Another purpose of this study was to derive a QSAR model using MLR for a series of 2-phenylbenzofuran derivatives (Fig. 6, Table 8). The success of QSAR models depends on what parameters are selected. Using quantum descriptors in QSAR models has the advantage of providing researchers with the electron density properties of molecular systems.

QSARs Results

Dataset for analysis. Antiplasmodial activity: The dataset was randomly divided into a training set of 40 compounds, reported in Table 9. Nine compounds (*i.e.*, 1, 3, 4, 6, 11, 12, 14, 35, and 47) were identified as outliers and excluded.

Cytotoxicity in mammals: Similarly, the dataset was divided into a training set of 40 compounds, reported in Table 10. Nine compounds (1, 8, 11, 23, 25, 28, 32, 46, and 49) were identified as outliers and excluded.

Multiple linear regression (MLR). Antiplasmodial activity: The training set compounds were used to develop a QSAR model. The correlation between the biological activities and descriptors was calculated using the following equation:

$$\log\left(\frac{1}{IC_{50}}\right) = 301.6 - 245.5D1 + 4.55Q4 + 1.75Q11 + 0.4585\log P + 0.000016\beta + 145.9Q8 \quad (10)$$

Equation (10) includes six parameters, namely, the bond lengths D1 (C1-C2), atomic net charges (Q4, Q11, Q8), log of the octanol/water partition coefficient (logP), and first-order hyperpolarizability (β). The 6-parameter model was

found to yield satisfactory correlation coefficient ($R^2 = 0.786$), adjusted squared correlation coefficient ($R^2_{adj} = 0.726$) and standard deviation (SD = 0.296). The result showed that compound 32, with an error value (difference between the estimated and observed activity values) of -0.477, was the most potent derivative among the studied derivatives. In general, molecules 32, 15, 41 were found to be the most potent derivatives, with their estimated activity values (4.079, 5.196, and 4.669) corresponding to their observed activity values (3.602, 4.771, and 4.255) and their error values (-0.477, -0.424, and -0.413, respectively). Compound 28 was found to be the least potent derivative, showing the largest gap between the observed and estimated biological activity values (error value = 0.452). On the basis of the observed and estimated activity values, it can be concluded that the final QSAR model is statistically significant and is verified by strong correlations.

Study of Cytotoxicity In mammals

The training set compounds were used to develop the QSAR model. The correlation between the biological activities and descriptors was calculated by the following equation:

$$\log\left(\frac{1}{IC_{50}}\right) = 19.13 + 1.173E_{HOMO} + 13.30Q5 - 0.1965HE - 0.1426S + 0.07960ZPVE - 0.000106\beta \quad (11)$$

Equation (11) includes six parameters, namely, the atomic net charge (Q5), highest occupied molecular orbital energy (E_{HOMO}), log of the octanol/water partition coefficient (logP), first-order hyperpolarizability (β), hydration energy (HE), entropy (S), and ZPVE. The 6-parameter model yields satisfactory correlation coefficient ($R^2 = 0.843$), adjusted squared correlation coefficient ($R^2_{adj} = 0.815$), and standard deviation (SD = 0.248). Compound 4, with an error value of -0.387, was found to be the most potent compound in the series of compounds, followed by compounds 4 and 17. Compounds 47, 38, and 44, with 8.215/8.219, 8.033/7.995, and 8.344/8.271 $\log(1/IC_{50})$ values, respectively, had acceptable error values of -0.003, 0.038, and 0.073 for the observed and estimated activities. Compound 34 was found to be the least potent compound, showing the greatest gap between the observed and estimated values

Table 9. The Calculated Parameters of the 40 Studied Molecules

Compounds	log(1/IC ₅₀) ^b		D1 (Å)	β (u.a)	Q4	Q8	Q11	logP
	Obs. ^c	Est. ^d						
2	4.863	4.545	1.390	2971.301	-0.113	0.302	-0.205	3.660
5	4.519	4.674	1.390	736.676	-0.111	0.303	-0.208	3.710
7	4.785	4.837	1.390	2728.817	-0.110	0.301	-0.201	4.650
8	4.279	4.517	1.390	1100.269	-0.129	0.308	-0.099	1.330
9	5.520	5.448	1.390	1364.969	-0.127	0.305	-0.112	3.660
10	4.881	4.625	1.390	463.082	-0.111	0.305	-0.095	2.290
13	5.037	4.673	1.390	3956.921	-0.216	0.306	-0.200	2.290
15	4.771	5.196	1.390	1379.944	-0.220	0.304	-0.104	3.640
16	5.312	5.105	1.390	2022.101	-0.217	0.307	-0.096	2.290
17	3.778	4.051	1.390	2029.587	-0.114	0.302	-0.224	1.080
18	4.681	4.779	1.390	3186.011	-0.099	0.301	-0.205	3.410
19	4.505	4.172	1.390	2522.079	-0.097	0.301	-0.200	2.030
20	4.672	4.416	1.390	1838.403	-0.116	0.304	-0.224	1.050
21	4.748	5.091	1.390	2987.481	-0.100	0.303	-0.205	3.380
22	4.342	4.484	1.390	2254.922	-0.098	0.303	-0.200	2.000
23	4.785	4.473	1.390	2266.749	-0.117	0.303	-0.253	0.760
24	5.491	5.291	1.390	3604.265	-0.102	0.301	-0.233	3.090
25	4.477	4.594	1.390	3173.766	-0.100	0.302	-0.228	1.720
26	3.477	3.286	1.390	1766.421	-0.130	0.303	-0.251	1.080
27	4.301	4.635	1.390	3155.619	-0.115	0.301	-0.231	3.410
28	4.491	4.040	1.390	2564.410	-0.113	0.302	-0.226	2.030
29	4.602	4.468	1.390	1107.845	-0.131	0.306	-0.125	1.080
30	5.398	5.454	1.390	1179.474	-0.129	0.304	-0.139	3.410
31	4.813	4.494	1.390	583.686	-0.113	0.303	-0.121	2.030
32	3.602	4.079	1.390	2187.813	-0.130	0.302	-0.253	1.050
33	4.447	4.712	1.390	3634.852	-0.114	0.300	-0.233	3.380
34	3.778	4.128	1.390	3190.204	-0.113	0.301	-0.228	2.000
36	5.713	5.480	1.390	1408.316	-0.129	0.303	-0.139	3.380
37	4.362	4.508	1.390	576.952	-0.113	0.302	-0.121	2.000
38	4.301	4.537	1.390	2292.549	-0.241	0.306	-0.251	1.080
39	5.314	5.484	1.390	2014.078	-0.245	0.306	-0.255	3.410
40	4.886	4.924	1.390	4177.548	-0.218	0.305	-0.226	2.030
41	4.255	4.669	1.390	866.973	-0.221	0.306	-0.126	1.080
42	5.467	5.351	1.390	943.570	-0.221	0.303	-0.131	3.410
43	4.869	5.166	1.390	1583.441	-0.218	0.306	-0.121	2.030
44	4.845	4.531	1.390	2812.163	-0.241	0.305	-0.253	1.050
45	5.776	5.509	1.390	2525.747	-0.244	0.305	-0.257	3.380
46	4.991	4.977	1.390	5042.692	-0.217	0.305	-0.228	2.000
48	5.803	5.354	1.390	1295.468	-0.221	0.302	-0.132	3.380
49	5.013	5.195	1.390	1968.340	-0.218	0.305	-0.122	2.000

^cObserved. ^dEstimated.

Table 10. The Calculated Parameters of the 40 Studied Molecules

Compounds	log(1/IC ₅₀) ^a		E _{HOMO} (eV)	β (u.a)	Q5	HE (Kcal mol ⁻¹)	S (Cal mol ⁻¹ -Kelvin)	ZPVE (Kcal mol ⁻¹)
	Obs ^c	Est ^d						
2	8.297	8.342	-4.847	2971.301	-0.188	-10.640	182.789	272.493
3	7.599	7.706	-4.755	2156.541	-0.183	-8.620	152.883	212.569
4	6.826	7.213	-4.864	566.127	-0.184	-12.570	177.928	241.189
5	6.519	6.561	-4.623	736.676	-0.193	-13.850	153.312	183.862
6	6.785	6.562	-4.839	4696.310	-0.184	-10.600	168.926	226.848
7	7.773	7.551	-4.780	2728.817	-0.183	-10.600	164.115	226.972
9	8.299	8.148	-4.996	1364.969	-0.213	-11.640	183.343	272.797
10	7.530	7.812	-4.762	463.082	-0.184	-8.470	153.069	212.607
12	8.299	8.039	-4.955	2181.151	-0.226	-11.640	182.635	272.822
13	6.653	6.955	-4.707	3956.921	-0.229	-8.560	152.841	212.599
14	8.117	7.910	-4.836	1136.588	-0.228	-19.940	138.604	169.070
15	8.301	8.443	-4.926	1379.944	-0.228	-11.960	180.781	272.527
16	7.107	7.245	-4.687	2022.101	-0.229	-8.480	152.357	212.649
17	7.487	7.818	-5.036	2029.587	-0.235	-22.350	150.947	189.375
18	8.279	7.921	-4.729	3186.011	-0.213	-11.150	195.951	292.266
19	7.299	7.363	-4.666	2522.079	-0.208	-9.020	165.055	232.475
20	8.265	8.352	-5.063	1838.403	-0.238	-26.920	143.566	172.091
21	8.267	8.593	-4.743	2987.481	-0.216	-15.370	187.235	275.030
22	8.307	7.818	-4.705	2254.922	-0.211	-13.450	157.917	215.133
24	8.253	8.318	-4.584	3604.265	-0.217	-17.950	194.691	277.333
26	8.196	8.234	-4.968	1766.421	-0.210	-21.420	149.863	189.401
27	7.992	8.288	-4.659	3155.619	-0.189	-10.260	194.979	292.254
29	8.253	8.151	-4.846	1107.845	-0.210	-20.560	150.617	189.164
30	8.253	8.072	-4.895	1179.474	-0.214	-11.280	195.322	292.619
31	7.489	7.715	-4.658	583.686	-0.185	-8.150	165.074	232.466
33	8.262	8.550	-4.687	3634.852	-0.190	-13.520	187.355	274.995
34	8.176	7.664	-4.655	3190.204	-0.184	-11.520	158.481	215.033
35	8.336	8.426	-4.872	1246.489	-0.210	-23.940	143.354	171.823
36	8.255	8.433	-4.905	1408.316	-0.214	-14.660	187.523	275.317
37	8.299	7.984	-4.673	576.952	-0.185	-11.550	158.068	215.136
38	8.033	7.995	-4.896	2292.549	-0.227	-21.350	150.102	189.367
39	8.258	8.068	-4.811	2014.078	-0.228	-11.260	194.126	292.630
40	6.643	6.810	-4.579	4177.548	-0.230	-8.060	165.007	232.454
41	8.107	7.974	-4.666	866.973	-0.230	-19.590	150.267	188.990
42	8.243	8.048	-4.756	943.570	-0.229	-9.420	192.747	292.403
43	7.045	7.158	-4.576	1583.441	-0.230	-8.150	164.711	232.466
44	8.344	8.271	-4.916	2812.163	-0.227	-24.920	142.856	172.055
45	8.262	8.323	-4.828	2525.747	-0.228	-14.510	186.661	275.385
47	8.215	8.219	-4.678	1043.430	-0.230	-22.960	143.269	171.632
48	8.272	8.146	-4.776	1295.468	-0.229	-12.810	186.619	275.049

^cObserved. ^dEstimated.

Table 11. The Correlation Matrix for the Six Descriptors Used in Eq. (10)

Descriptors	D1	β	Q4	Q8	Q11	LogP
D1	1					
β	-0.172	1				
Q4	0.684	-0.0047	1			
Q8	-0.239	-0.238	-0.620	1		
Q11	0.120	-0.654	-0.080	0.342	1	
logP	0.223	0.056	0.053	-0.323	0.135	1

Table 12. The Correlation Matrix for the Six Descriptors Used in Eq. (11)

Descriptors	E_{HOMO}	β	Q5	HE	S	ZPVE
E_{HOMO}	1					
B	0.179	1				
Q5	0.236	0.032	1			
HE	0.477	0.160	0.400	1		
S	0.068	0.217	0.075	0.476	1	
ZPVE	0.088	0.220	0.072	0.578	0.984	1

Table 12. Cross-Validation of Eq. (10_

Training Set	N	R^2	R^2_{adj}	Test set	N	R^2	R^2_{adj}
A + B	27	0.836	0.786	C	13	0.692	0.384
A + C	27	0.812	0.755	B	13	0.904	0.800
B + C	26	0.667	0.563	A	14	0.893	0.802
Average		0.772	0.702			0.828	0.662

(error value = 0.512). The success of the study model in this section can be attributed to the uniformity of the chemical structures of the scaffolds. In addition, the model could be used to develop new drugs with higher efficacy compared to standard drugs. A correlation matrix was used to correlate biological activities with various variables (Tables 11 and 12).

Internal validation. Antiplasmodial activity: To validate the developed model (Eq. (10)), internal validation was performed using the leave-one-out, with a coefficient of $R^2_{\text{cv}} = 0.659$, and the leave-many-out procedures based on the following steps.

First, the experimental data values were divided into three subsets (*i.e.*, A, B, and C). The molecules with the numbers $n * 3 + 1$ were assigned to the first subset (A), those with the numbers $n * 3 + 2$ to the second subset (B), and those with the numbers $n * 3 + 3$ to the third subset (C), with n varying from 0 to 14.

Secondly, three pairs (*i.e.*, A + B, A + C, and B + C) were obtained by combining two of the three subsets at each time, and the correlation equation was derived with the same descriptors. The resulting equation was used to predict the data for the remaining subsets. It was found that the predicted values, which were obtained using R^2 for the

Table 13. Cross-Validation of Eq. (11)

Training set	N	R ²	R ² _{adj}	Test set	N	R ²	R ² _{adj}
A + B	27	0.886	0.852	C	13	0.865	0.731
A + C	27	0.858	0.816	B	13	0.908	0.816
B + C	26	0.808	0.747	A	14	0.924	0.858
Average		0.851	0.805			0.899	0.802

subsets A + B, A + C, and B + C, were very close to those of the full training set (A + B + C) and that the mean values of R² for the training set were also close to those of R² for the test set (Tables 12 and 13). The R² values of the models corresponding to A + B, A + C, and B + C subsets were closer to 0.80, indicating that the developed model is stable and can be used efficiently to evaluate the antiplasmodial activity of other molecules for which experimental data are not available.

Study of cytotoxicity in mammals: To validate the second model (Eq. (11)), internal validation was performed using the leave-one-out method, with a coefficient of R²_{cv} = 0.763, and the leave-many-out methods.

Figures 7 and 8 show the linear correlation, obtained using Equations (10) and (11), respectively, between the observed and predicted values of the activities mentioned in Tables 9 and 10.

CONCLUSIONS

The molecular geometries of 2-phenylbenzofuran in the ground state were determined using the GGA-PBE, PBV86, and meta-GGA-TPSS functionals with the 6-31G(d,p) basis set. The calculated values of the dipole moment and first-order hyperpolarizability indicated that 2-phenylbenzofuran and its derivatives had a quite good NLO behavior. In addition, the predicted NLO properties of 2-phenylbenzofuran and its derivatives exhibited interesting compared to those of other materials. Therefore, it can be concluded that all the compounds under study are good candidates for the development of second-order NLO materials. Furthermore, the results show that quantum chemistry descriptors, namely, the energies of highest occupied molecular orbit E_{HOMO}, natural charge, bond lengths, first-order hyperpolarizability, entropy, ZPVE, log

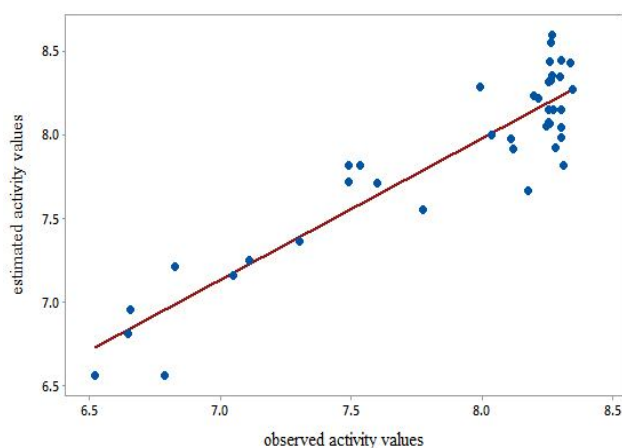


Fig. 7. The QSAR model plot of correlations representing the observed vs. estimated log(1/IC₅₀) values for cytotoxicity in mammals.

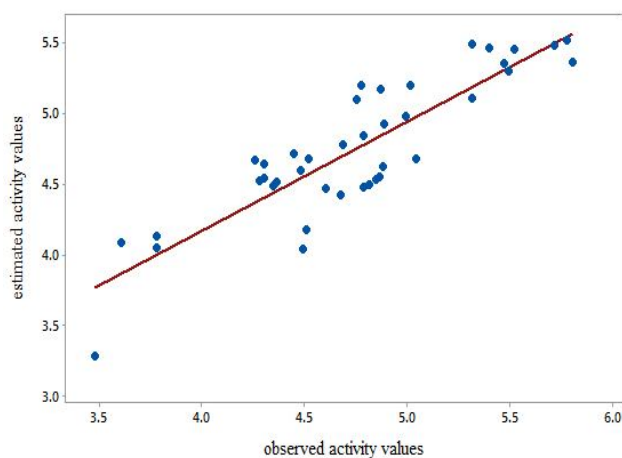


Fig. 8. The QSAR model plot of correlations representing the observed vs. estimated log(1/IC₅₀) values for antiplasmodial activity.

octanol/water partition coefficient, and hydration energy, are useful in predicting biological activities. The two QSAR models (Eqs. (10) and (11)) developed in the present study were used effectively to calculate the activities of 2-phenylbenzofuran derivatives for which experimental data were unavailable. The above two models can also describe approximately 81% of the variance in activities of other compounds. The results may vary depending on the random nature of the algorithm in selecting descriptors. When descriptors are selected with minor significance, overfitting may occur. However, this does not change the fact that the first-order hyperpolarizability is a very good descriptor for QSAR models.

REFERENCES

- [1] Aslam, S. N.; Stevenson, P. C.; Kokubun, T.; Hall, D. R., Antibacterial and antifungal activity of cicerfuran and related 2-arylbenzofurans and stilbenes, *Microbiol. Res.* **2009**, *164*, 191-195, DOI: 10.1016/j.micres.2006.11.012.
- [2] Galal, S. A.; Abd El-All, A. S.; Abdallah, M. M.; El-Diwani, H. I., Synthesis of potent antitumor and antiviral benzofuran derivatives, *Bioorganic Med. Chem. Lett.* **2009**, *19*, 2420-2428, DOI: 10.1016/j.bmcl.2009.03.069.
- [3] Khan, M. W.; Alam, M. J.; Rashid, M.; Chowdhury, R., A new structural alternative in benzo [b] furans for antimicrobial activity, *Bioorg. Med. Chem.* **2005**, *13*, 4796-4805, DOI: 10.1016/j.bmc.2005.05.009.
- [4] Manna, K.; Agrawal, Y. K., Design, synthesis, and antitubercular evaluation of novel series of 3-benzofuran-5-aryl-1-pyrazolyl-pyridylmethanone and 3-benzofuran-5-aryl-1-pyrazolylcarbonyl-4-oxo-naphthyridin analogs, *Eur. J. Med. Chem.* **2010**, *45*, 3831-3839, DOI: 10.1016/j.ejmech.2010.05.035.
- [5] Rida, S. M.; El-Hawash, S. A.; Fahmy, H. T.; Hazza, A. A.; El-Meligy, M. M., Synthesis and in vitro evaluation of some novel benzofuran derivatives as potential anti-HIV-1, anticancer, and antimicrobial agents, *Arch. Pharm. Res.* **2006**, *29*, 16-25, DOI: 10.1007/BF02977463.
- [6] Xie, Y. -S.; Kumar, D.; Bodduri, V. V., *et al.* Microwave-assisted parallel synthesis of benzofuran-2-carboxamide derivatives bearing anti-inflammatory, analgesic and antipyretic agents, *Tetrahedron Lett.* **2014**, *55*, 2796-2800, DOI: 10.1016/j.tetlet.2014.02.116.
- [7] Ono, M.; Kawashima, H.; Nonaka, A., *et al.* Novel benzofuran derivatives for PET imaging of β -amyloid plaques in Alzheimer's disease brains, *J. Med. Chem.* **2006**, *49*, 2725-2730, DOI: 10.1021/jm051176k.
- [8] Ragab, F. A.; Tawfeek, H., Synthesis, inotropic, anti-arrhythmic and hypotensive activities of some new benzofuran derivatives, *Eur. J. Med. Chem.* **1987**, *22*, 265-267, DOI: 10.1016/j.ejmech.2009.02.012.
- [9] Bakunova, S. M.; Bakunov, S. A.; Wenzler, T., *et al.* Synthesis and *in vitro* antiprotozoal activity of bisbenzofuran cations, *J. Med. Chem.* **2007**, *50*, 5807-5823, DOI: 10.1021/jm0708634.
- [10] Bakunov, S. A.; Bakunova, S. M.; Wenzler, T., *et al.* Synthesis and antiprotozoal activity of cationic 2-phenylbenzofurans, *J. Med. Chem.* **2008**, *51*, 6927-6944, DOI: 10.1021/jm800918v.
- [11] Bakunov, S. A.; Bakunova, S. M.; Bridges, A. S., *et al.* Synthesis and antiprotozoal properties of pentamidine congeners bearing the benzofuran motif, *J. Med. Chem.* **2009**, *52*, 5763-5767, DOI: 10.1021/jm9006406.
- [12] Satheeshchandra, S.; Haleshappa, D.; Rohith, S.; Jayarama, A.; Shetty, N., Novel benzofuran based chalcone material for potential nonlinear optical application, *Phys. B: Condens. Matter.* **2019**, *560*, 191-196, DOI: 10.1016/j.physb.2019.02.014.
- [13] Zhang, C. -R.; Liu, Z. -J.; Chen, Y. -H.; Ma, J.; Chen, H. -S.; Zhang, M. -L., Density functional theory study on organic dye sensitizers containing bis-dimethylfluorenyl amino benzofuran, *Chinese J. Chem. Phys.* **2009**, *22*, 489, DOI: 10.1088/1674-0068/22/05/489-496.
- [14] Hwu, J. R.; Chuang, K. -S.; Chuang, S. H.; Tsay, S. -C., New benzo [b] furans as electroluminescent materials for emitting blue light, *Org. Lett.* **2005**, *7*, 1545-1548, DOI: 10.1021/ol050196d.
- [15] Oter, O.; Ertekin, K.; Kirilmis, C.; Koca, M.; Ahmedzade, M., Characterization of a newly synthesized fluorescent benzofuran derivative and usage as a selective fiber optic sensor for Fe(III), *Sens. Actuators B Chem.* **2007**, *122*, 450-456, DOI:

- 10.1016/j.snb.2006.06.010.
- [16] Migalska-Zalas, A.; Korchi, K. E.; Chtouki, T., Enhanced nonlinear optical properties due to electronic delocalization in conjugated benzodifuran derivatives, *Opt. Quantum Electron.* **2018**, *50*, 1-10, DOI: 10.1007/s11082-018-1659-x.
- [17] Maridevarmath, C.; Naik, L.; Negalurmth, V.; Basanagouda, M.; Malimath, G., Synthesis, photophysical, DFT and solvent effect studies on biologically active benzofuran derivative: (5-Methyl-benzofuran-3-yl)-acetic acid hydrazide, *Chem. Data Coll.* **2019**, *21*, 100221, DOI: 10.1016/j.cdc.2019.100221.
- [18] Hiremath, S. M.; Patil, A. S.; Hiremath, C. S., *et al.* Structural, spectroscopic characterization of 2-(5-methyl-1-benzofuran-3-yl) acetic acid in monomer, dimer and identification of specific reactive, drug likeness properties: experimental and computational study, *J. Mol. Struct.* **2019**, *1178*, 1-17, DOI: 10.1016/j.molstruc.2018.10.007
- [19] Murthy, P. K.; Krishnaswamy, G.; Armaković, S., *et al.* Structural and spectroscopic characterization, reactivity study and charge transfer analysis of the newly synthesized 2-(6-hydroxy-1-benzofuran-3-yl) acetic acid, *J. Mol. Struct.* **2018**, *1162*, 81-95, DOI: 10.1016/j.molstruc.2018.02.081.
- [20] Hasan, T.; Mehdi, S. H.; Ghalib, R. M.; Singh, P.; Misra, N., An investigation on structural, vibrational and nonlinear optical behavior of 4b,9b-dihydroxy-7, 8-dihydro-4bH-Indeno [1,2-b] benzofuran-9,10(6H, 9bH)-dione: A DFT study, *J. Chem. Sci.* **2015**, *127*, 2217-2223, DOI: 10.1007/s12039-015-0984-x.
- [21] Singh, V., *Ab initio* and DFT studies of the vibrational spectra of benzofuran and some of its derivatives, *Spectrochim. Acta A Mol. Biomol. Spectrosc.* **2006**, *65*, 1125-1130, DOI: 10.1016/j.saa.2006.01.045.
- [22] Islam, M. M.; Akther, T.; Ikejiri, Y., *et al.* Synthesis, structural properties, electrophilic substitution reactions and DFT computational studies of calix [3] benzofurans, *RSC Adv.* **2016**, *6*, 50808-50817, DOI: 10.1039/C6RA06219A.
- [23] Aggarwal, K.; Khurana, J. M., Synthesis of a novel 5a, 10a-dihydroxy-5aH-[1,3] dioxolo [4,5-f] indeno [1,2-b] benzofuran-10(10aH)-one their XRD, FTIR, NMR and DFT studies, *J. Mol. Struct.* **2017**, *1130*, 739-747, DOI: 10.1016/j.molstruc.2016.11.008.
- [24] Xue, Y.; Liu, Y.; An, L., *et al.* Electronic structures and spectra of quinoline chalcones: DFT and TDDFT-PCM investigation, *Comput. Theor. Chem.* **2011**, *965*, 146-153, DOI: 10.1016/j.comptc.2011.01.042.
- [25] Benhalima, N.; Boukabcha, N.; Tamer, Ö., *et al.* Solvent effects on molecular structure, vibrational frequencies, and NLO properties of N-(2, 3-dichlorophenyl)-2-nitrobenzene-sulfonamide: a density functional theory study, *Braz. J. Phys.* **2016**, *46*, 371-383, DOI: 10.1007/s13538-016-0419-2.
- [26] Altürk, S.; Boukabcha, N.; Benhalima, N., *et al.* Conformational, spectroscopic and nonlinear optical investigations on 1-(4-chlorophenyl)-3-(4-chlorophenyl)-2-propen-1-one: a DFT study, *Indian J Phys.* **2017**, *91*, 501-511, DOI: 10.1007/s12648-016-0945-3.
- [27] Kourat, O.; Djafri, A.; Benhalima, N., *et al.* Synthesis, crystal structure, Hirshfeld surface analysis, spectral characterization, reduced density gradient and nonlinear optical investigation on (E)-N'-(4-nitrobenzylidene)-2-(quinolin-8-yloxy) acetohydrazide monohydrate: A combined experimental and DFT approach, *J. Mol. Struct.* **2020**, *1222*, 128952, DOI: 10.1016/j.molstruc.2020.128952.
- [28] Aouidate, A.; Ghaleb, A.; Ghamali, M., *et al.* Combining DFT and QSAR studies for predicting psychotomimetic activity of substituted phenethylamines using statistical methods, *J. Taibah Univ. Sci.* **2016**, *10*, 787-796, DOI: 10.1016/j.jtusci.2016.07.001.
- [29] Rahmouni, A.; Touhami, M.; Benaissa, T. Fukui Indices as QSAR Model Descriptors: The Case of the Anti-HIV Activity of 1-2-[(Hydroxyethoxy) Methyl]-6-(Phenylthio) Thymine Derivatives, *I. J. Chemoinform. Chem. Eng. (IJCCE)*. **2017**, *6*, 31-44, DOI: 10.4018/IJCCE.2017070103.
- [30] Boudergua, S.; Alloui, M.; Belaidi, S.; Al Mogren, M. M.; Ibrahim, U. A. E.; Hochlaf, M., QSAR modeling and drug-likeness screening for antioxidant activity of benzofuran derivatives, *J. Mol. Struct.* **2019**, *1189*, 307-314, DOI: 10.1016/j.molstruc.2019.04.004.
- [31] Oluwaseye, A.; Uzairu, A.; Shallangwa, G. A.; Abechi,

- S. E., Quantum chemical descriptors in the QSAR studies of compounds active in maxima electroshock seizure test, *J. King Saud Univ. Sci.* **2020**, *32*, 75-83, DOI: 10.1016/j.jksus.2018.02.009.
- [32] Ekins, S.; Mestres, J.; Testa, B., In silico pharmacology for drug discovery: methods for virtual ligand screening and profiling, *Br. J. Pharmacol.* **2007**, *152*, 9-20, DOI: 10.1038/sj.bjp.0707306.
- [33] Montgomery, D. C.; Peck, E. A.; Vining, G. G., Introduction to Linear Regression Analysis: John Wiley & Sons, **2021**.
- [34] Topliss, J. G.; Edwards, R. P., Chance factors in studies of quantitative structure-activity relationships, *J. Med. Chem.* **1979**, *22*, 1238-1244, DOI: 10.1021/jm00196a017.
- [35] Wold, S., PLS for Multivariate Linear Modeling. QSAR: Chemometric Methods in Molecular Design Methods and Principles in Medicinal Chemistry). Weinheim, Germany: Verlag-Chemie, **1994**.
- [36] Eriksson, L.; Verhaar, H. J.; Hermens, J. L., Multivariate characterization and modeling of the chemical reactivity of epoxides, *Environ. Toxicol. Chem.* **1994**, *13*, 683-691, DOI: 10.1002/etc.5620130502.
- [37] Sandberg, M.; Eriksson, L.; Jonsson, J.; Sjöström, M.; Wold, S., New chemical descriptors relevant for the design of biologically active peptides. A multivariate characterization of 87 amino acids, *J. Med. Chem.* **1998**, *41*, 2481-2491, DOI: 10.1021/jm9700575.
- [38] Minitab, I., MINITAB Statistical Software, Minitab Release. **2000**, p. 13.
- [39] Frisch, A.; Dennington, I.; Keith, T., *et al.* Reference, Version 4.0, Gaussian Inc.). Pittsburgh, **2007**.
- [40] Frisch, M.; TRUCKS, G.; SCHLEGEL, H. Gaussian 09, Revision A02 [Z], Pittsburgh: Gaussian Inc. **2009**.
- [41] Heyd, J.; Scuseria, G. E.; Ernzerhof, M., Hybrid functionals based on a screened Coulomb potential, *J. Chem. Phys.* **2003**, *118*, 8207-8215, DOI: 10.1063/1.1564060.
- [42] Becke, A. D., Density-functional thermochemistry. I. The effect of the exchange-only gradient correction, *J. Chem. Phys.* **1992**, *96*, 2155-2160, DOI: 10.1063/1.462066.
- [43] Tao, J.; Perdew, J. P.; Staroverov, V. N.; Scuseria, G. E., Climbing the density functional ladder: Nonempirical meta-generalized gradient approximation designed for molecules and solids, *Phys. Rev. Lett.* **2003**, *91*, 146401, DOI: 10.1103/PhysRevLett.91.146401.
- [44] Staroverov, V. N.; Scuseria, G. E.; Tao, J.; Perdew, J. P., Comparative assessment of a new nonempirical density functional: Molecules and hydrogen-bonded complexes, *J. Chem. Phys.* **2003**, *119*, 12129-12137, DOI: 10.1063/1.1626543.
- [45] Hehre, W. J. *Ab initio* molecular orbital theory, *Acc. Chem. Res.* **1976**, *9*, 399-406, DOI: 10.1021/ar50107a003.
- [46] Pojarová, M.; Dušek, M.; Jančařík, A.; Makrlík, E.; Sedláková, Z., 2-(2-Methoxyphenyl)-1-benzofuran, *Acta Crystallogr. E.* **2011**, *67*, o1427-o1427, DOI: 10.1107/S1600536811017168.
- [47] Uzun, S.; Demircioğlu, Z.; Taşdoğan, M.; Ağar, E., Quantum chemical and X-ray diffraction studies of (E)-3-(((3,4-dimethoxybenzyl) imino) methyl) benzene-1, 2-diol, *J. Mol. Struct.* **2020**, *1206*, 127749, DOI: 10.1016/j.molstruc.2020.127749
- [48] Ekici, Ö.; Demircioğlu, Z.; Ersanlı, C. C.; Çukurovalı, A., Experimental and theoretical approach: Chemical activity, charge transfer of DNA/ECT, thermodynamic, spectroscopic, structural and electronic properties of N-(4-(3-methyl-3-phenylcyclobutyl) thiazol-2-yl) acetamide molecule, *J. Mol. Struct.* **2020**, *1204*, 127513, DOI: 10.1016/j.molstruc.2019.127513.
- [49] Sethi, A.; Prakash, R., Novel synthetic ester of Brassicasterol, DFT investigation including NBO, NLO response, reactivity descriptor and its intramolecular interactions analyzed by AIM theory, *J. Mol. Struct.* **2015**, *1083*, 72-81, DOI: 10.1016/j.molstruc.2014.11.028.
- [50] Reed, A. E.; Weinhold, F., Natural bond orbital analysis of near-Hartree-Fock water dimer, *J. Chem. Phys.* **1983**, *78*, 4066-4073, DOI: 10.1063/1.445134.
- [51] Benhalima, N.; Yahiaoui, S.; Boubegra, N., *et al.* Quantum chemical investigation of spectroscopic, electronic and NLO properties of (1E, 4E)-1-(3-nitrophenyl)-5-phenylpenta-1,4-dien-3-one, *Int. J. Adv. Chem.* **2018**, *6*, 121-131,

- DOI: 10.14419/ijac.v6i1.11795.
- [52]Stratmann, R. E.; Scuseria, G. E.; Frisch, M.J., An efficient implementation of time-dependent density-functional theory for the calculation of excitation energies of large molecules, *J. Chem. Phys.* **1998**, *109*, 8218-8224, DOI: 10.1063/1.477483.
- [53]Cossi, M.; Rega, N.; Scalmani, G.; Barone, V., Energies, structures, and electronic properties of molecules in solution with the C-PCM solvation model, *J. Comput. Chem.* **2003**, *24*, 669-681, DOI: 10.1002/jcc.10189.
- [54]O'boyle, N. M.; Tenderholt, A. L.; Langner, K. M., cclib: A library for package-independent computational chemistry algorithms, *J. Comput. Chem.* **2008**, *29*, 839-845. DOI: 10.1002/jcc.20823.
- [55]Parr, R. G.; Szentpály, L. V.; Liu, S., Electrophilicity index, *J. Am. Chem. Soc.* **1999**, *121*, 1922-1924, DOI: 10.1021/ja983494x.
- [56]Padmanabhan, J.; Parthasarathi, R.; Subramanian, V.; Chattaraj, P., Electrophilicity-based charge transfer descriptor, *J. Phys. Chem. A.* **2007**, *111*, 1358-1361, DOI: 10.1021/jp0649549.
- [57]Padmanabhan, J.; Parthasarathi, J. R.; Subramanian, V.; Chattaraj, P., Chemical reactivity indices for the complete series of chlorinated benzenes: Solvent effect, *J. Phys. Chem. A.* **2006**, *110*, 2739-2745, DOI: 10.1021/jp056630a.
- [58]Nazari, F. ; Zali, F. R., Density functional study of the relative reactivity of the carbonyl group in substituted cyclohexanone, *J. Mol. Struct. -THEOCHEM.* **2007**, *817*, 11-18, DOI: 10.1016/j.theochem.2007.04.013.
- [59]Kleinman,D. Nonlinear Dielectric Polarization in Optical Media, *Phys. Rev.* **1962**, *126*, 1977, DOI: 10.1103/PhysRev.126.1977.
- [60]Cassidy, C.; Halbout, J.; Donaldson, W.; Tang, C. Nonlinear optical properties of urea, *Opt. Commun.* **1979**, *29*, 243-246, DOI: 10.1016/0030-4018(79)90027-0.
- [61]Li, F.; Wu, H.; Li, L.; Li, X.; Zhao, J.; Peijnenburg, W. J., Docking and QSAR study on the binding interactions between polycyclic aromatic hydrocarbons and estrogen receptor, *Ecotoxicol. Environ. Saf.* **2012**, *80*, 273-279, DOI: 10.1016/j.ecoenv.2012.03.009.